Transparent mm-Wave Array on a Glass Substrate with Surface Wave Reduction

Rodriguez Cano, Rocio; Zhang, Shuai; Pedersen, Gert Frølund

Published in:
2020 14th European Conference on Antennas and Propagation (EuCAP)

DOI (link to publication from Publisher):
10.23919/EuCAP48036.2020.9136095

Publication date:
2020

Document Version
Accepted author manuscript, peer reviewed version

Transparent mm-Wave Array on a Glass Substrate with Surface Wave Reduction

Rocío Rodríguez-Cano, Shuai Zhang, Gert F. Pedersen
Antenna, Propagation and Mm-Wave Systems Section (APMS), Department of Electronic Systems,
Aalborg University, Aalborg, Denmark
{*rrc, sz, gfp*}*@es.aau.dk*

***Abstract*—In this paper, a transparent dual-element millimeter-wave (mm-wave) array for handsets is proposed. The antenna is mounted on top of a glass display and it is made by diamond grid cells that provide a transparency of 86 %. In order to reduce the surface waves generated and make the radiation pattern more directive, several rows of meshed patches have been placed in front of the mm-wave bow-tie array. The antenna array operates from 26.5 to 29.5 GHz and has a total efficiency of more than 70 % in the operating bandwidth. The array is able to steer the beam 70° with a realized gain higher than 7 dBi.**

***Index Terms*—5G mobile communication, Antenna-on-Display, handset, transparent antenna.**

I. Introduction

New frequency bands have been introduced in the millimeter-wave (mm-wave) spectrum for the fifth generation of mobile communication (5G) [1]. For that reason, 5G-enabled handsets need to include antenna systems that cover the new bands. The limited available space in handsets has prompted the appearance of integrated low and high-frequency antennas [2]–[6] and new locations for the mm-wave antenna designs, where the antennas are printed on the active display region [7]–[10]. The glass display of the handset is employed as the substrate of the antenna. In [9], an optically invisible antenna is integrated within the OLED touch display of a smartwatch. In [10], a transparent Antenna-on-Display (AoD) solution are presented for handsets at 28 GHz. An optically invisible antenna and a transparent one are proposed in [7] for mm-wave frequencies. However, the total efficiency of the two antennas-on-display has low values: 29.83 % and 52.37 %, respectively.

One of the main challenges of planar antennas is the control of the surface waves. The appearance of surface waves is more noticeable with higher dielectric permittivity substrates, like glass [11]. There are several reasons why surface waves are detrimental to antennas: they distort the radiation pattern, increase the mutual coupling of the array and reduce the antenna efficiency. For those reasons, it is important to control the surface waves in the case of AoD.

One of the solutions proposed in literature to reduce the surface waves is to drill holes in the substrate to reduce the effective dielectric constant. However, since the mm-wave array is thought for antenna-on-display applications, the substrate cannot be perforated.

In this paper, a transparent array is presented to be placed on the handset display. Several layers of patches are located in front of the array to radiate the current coupled from the surface waves and thereby reduce their effect. The array achieves high radiation efficiency.

II. Antenna System Design

The handset is formed by a glass substrate and a metallic plane on the bottom. The transparent antenna system is printed on the top part of the display, as shown in Fig. 1. Since the aim of this work is to show the surface wave reduction, the array is located in the longest edge of the terminal. This manner, the surface waves have more space to propagate without finding any edges. However, this solution can be employed in different locations and with different phone form factors.

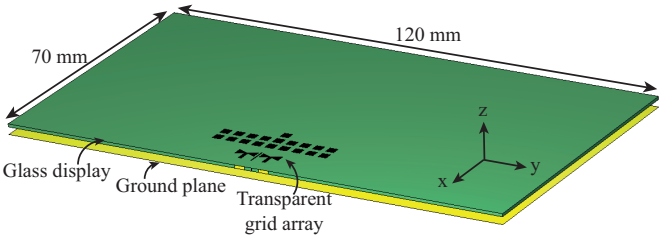

Fig. 1. Exploded view of the transparent array mounted on the handset.

The antenna system configuration is detailed in Fig. 2. The system is composed of 2 meshed bow-tie shaped monopoles. Since the bow-tie element provides high gain, only two antennas are needed so that the array gain is higher than 7 dBi in the frequency band. A strip is placed between the antenna elements to reduce the mutual coupling of the array. Since the aim is not to perforate the substrate, the strip is grounded on the edge of the glass. The structure proposed to reduce the surface waves consists of several row of meshed patches, as shown in Fig. 2(a). The patches, which are fed by the surface waves, radiate most of the energy coupled from the monopoles, preventing it to propagate along the substrate. The size of the square patches is $a = 2.1$ mm, $b = 1.785$ mm and $c = 1.575$ mm. The display is made of a glass substrate of $\epsilon_r = 6$ and thickness of 0.7 mm. The unit cell that constitutes the grid has a thickness of 2000 Å and a width of 5 μm. For that mesh width, the optical transparency is 86 % [7] and

the conductivity 2.675×10^6 S/m [12]. The dimensions of the grid are $w_{ver} = 100$ μm and $w_{hor} = 50$ μm (Fig. 2(b)). The grid cells can be implemented with a photolithography process, as shown in [7].

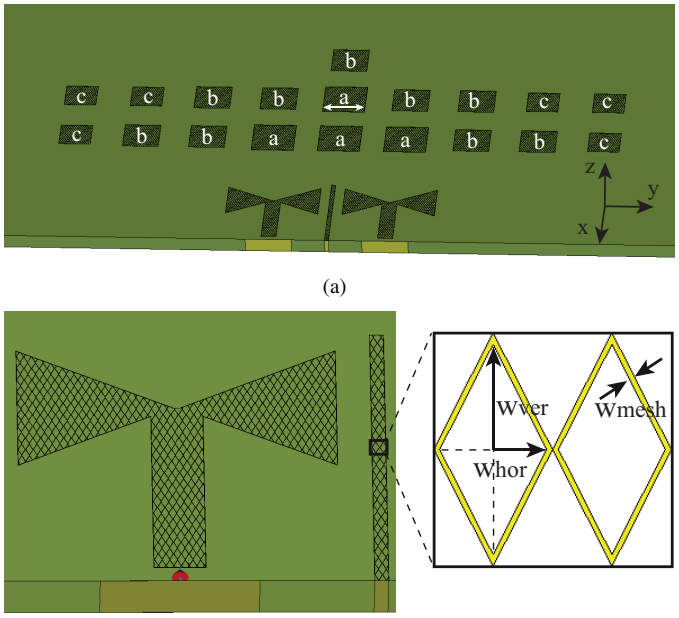

(a)

(b)

Fig. 2. Simulated models. (a) Antenna array with strip structure to reduce the surface waves. (b) Details of the mm-wave antenna and diamond grid.

III. Surface Wave Reduction

The effect of surface waves in the radiation pattern can be detrimental in systems that require very directive antennas. The radiation patterns of the array and the proposed solution with radiating strips to reduce surface waves are represented in Fig. 3. In the case of only the antenna array on the display, the main lobe gain is 7.6 dBi. The proposed array with strips can achieve 10.5 dBi.

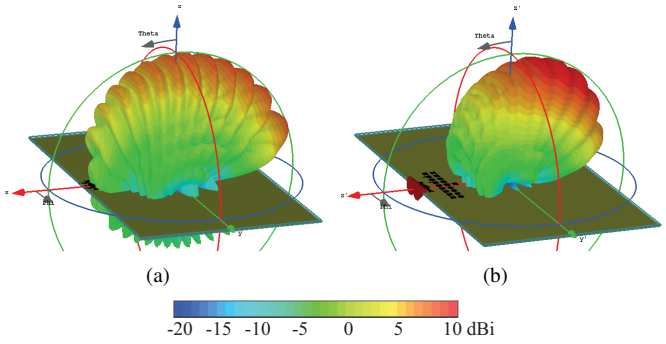

Fig. 3. 3D realized gain radiation pattern. (a) Antenna array without strips. (b) Antenna array with patch structure to reduce the surface waves.

The polar radiation patterns of both structures are represented in Fig. 4. As it can be seen in Fig. 4(a), the propagation of the surface wave causes the appearance of ripples in the radiation pattern. The value of the realized gain in boresight (-30°) is 5 dB. On the other hand, when the patches are placed in front of the array, there is a gain enhancement of 5 dBi and the radiation pattern is smoother. Besides, the back lobes are reduced 5 dBi. The 3 dB angular width in the $\phi = 0°$ cut is 8.4° and 48.1° for the array without and with patches respectively. The deep ripples in the radiation pattern are responsible for the large difference. The 3 dB angular width in the $\phi = 90°$ cut is 35.1° and 61.2°, respectively.

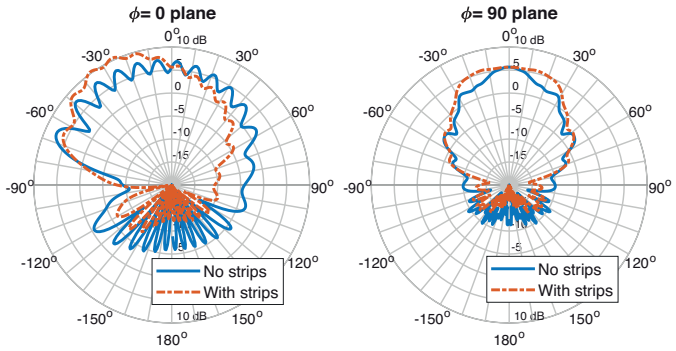

(a) (b)

Fig. 4. In-phase realized gain radiation pattern at 28 GHz. (a) $\Phi = 0°$ plane. (b) $\Phi = 90°$ plane.

For a better comprehension of the mechanism to reduce the surfaces waves, the surface currents of the proposed mm-wave array have been represented in Fig. 5 with and without the patches. When no patches are placed in front of the array (Fig. 5(a)), it can be seen how the surface wave propagates in the glass. The surface wave is more noticeable in the direction of the center of the array (-x axis). With only one row of patches, the current is still larger in that direction. Adding two rows of patches redirects the surface current in more directions. The last patch added in a third row allows to reduce considerably the surface current in the original direction (-x axis). In conclusion, the presence of the patches decreases the surface currents up to 15 dB and as it can be seen in Fig. 5(b) the surface waves are significantly reduced. This is due to the fact that the patches are fed by the surface currents. This allows the radiation of most of the energy.

IV. Array Performance

The simulations results are carried out by CST Microwave Studio 2019. The S-parameters of the array are plotted in Fig. 6. The reflection coefficient of the antenna is matched below -10 dB from 26.4 to 29.36 GHz. The transmission coefficient has been reduced with the presence of the grounded strip between the antennas, with a value lower than -13.2 dB in all the operating bandwidth. The total efficiency of the array is represented as well in Fig. 6. The efficiency is higher than 70 % in all the bandwidth and it reaches a value of 83 % in the frequency range 27.5-29 GHz.

The realized gain evolution as a function of the frequency in the boresight direction is plotted in Fig. 7. The realized gain is higher than 9 dBi in the operating frequency band.

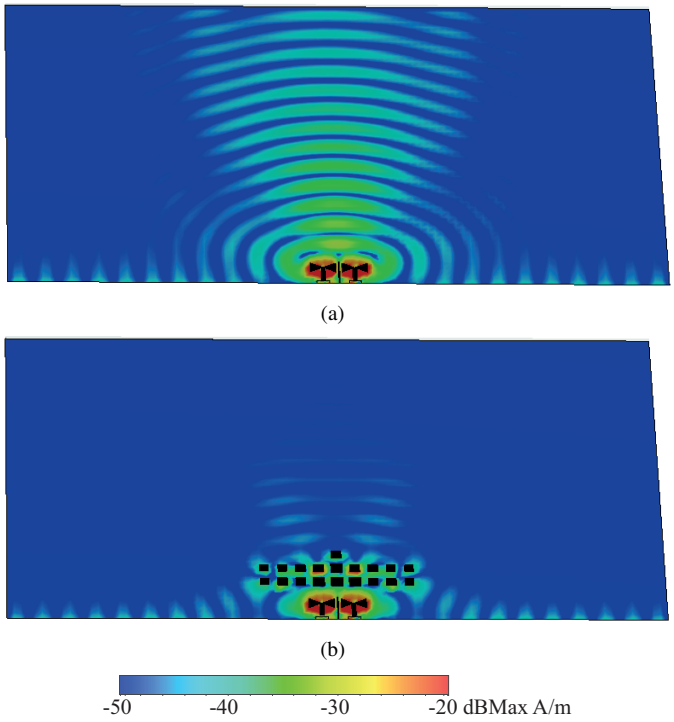

Fig. 5. Surface currents at 28 GHz. (a) Without patches. (b) With patches.

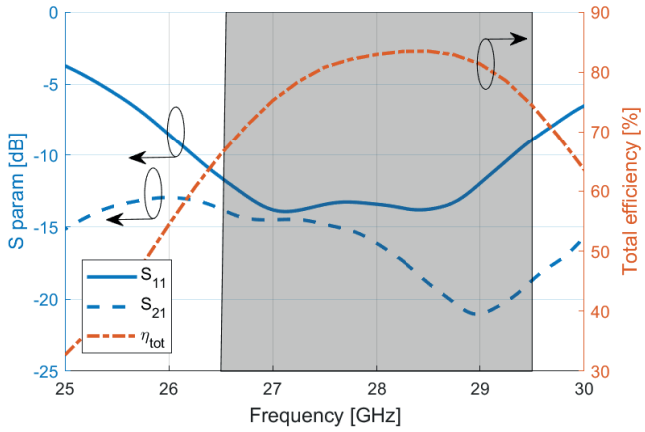

Fig. 6. S parameters of the proposed design and total efficiency of the array (including mismatching losses).

Since high gain antennas provide narrow beams, mm-wave arrays are required to steer the beam to provide wide coverage. One of the important figures of merit is the beam-steering envelope. It is calculated by selecting the beam that provides the maximum gain at every angle. The beam-steering envelope of 12 different beams is represented in Fig. 8. Since the direction of the main beam is tilted with respect to the axes of Fig. 2, the coordinate system has been rotated -25° (with the y axis fixed). The reason why the radiation pattern is tilted in the xz plane is due to the combination of structures with different radiation patterns. In other words, the bow-tie monopoles present an endfire radiation pattern, while the rows

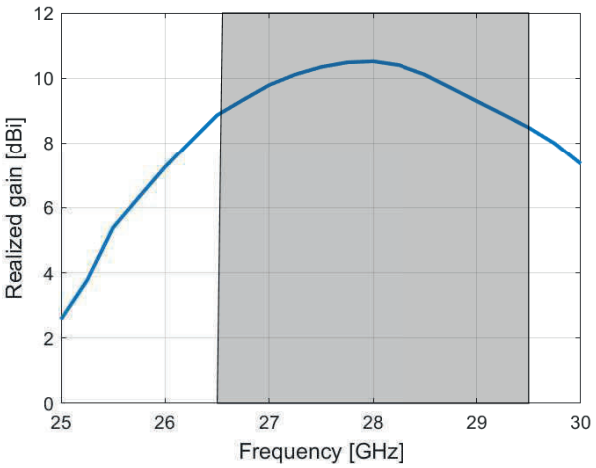

Fig. 7. Realized gain evolution in terms of frequency in the boresight direction.

of patches have broadside radiation. The maximum scanning angle for a realized gain higher than 7 dBi is $\theta = \pm 35°$.

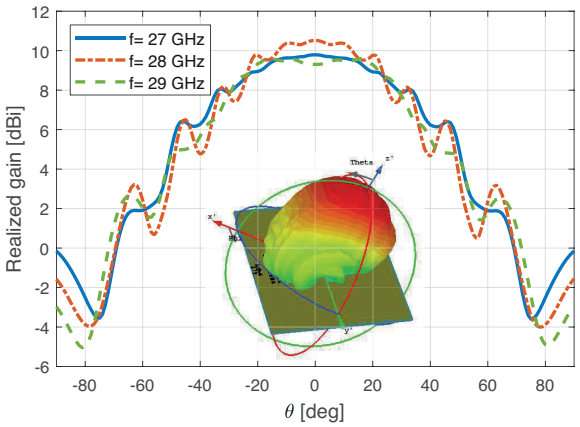

Fig. 8. Beam-steering envelope. The coordinate system has been rotated -25° (with the y axis fixed) with respect to the one in Fig. 2, to point at boresight.

V. Conclusion

A transparent mm-wave array has been designed for Antenna-on-Display applications. Several rows of patches have been places in front of the array to reduce the surface wave propagating in the glass substrate. This makes the radiation pattern more directive and with less ripples. The array operates in the frequency range 26.4-29.3 GHz and presents a total efficiency higher than 70 % in all the bandwidth. The array is able to beam-steer $\theta = \pm 35°$, with a gain higher than 7 dBi.

Acknowledgment

This work was supported by the InnovationsFonden project of Reconfigurable Arrays for Next Generation Efficiency (RANGE).

REFERENCES

[1] J. Lee, E. Tejedor, K. Ranta-aho, H. Wang, K.-T. Lee, E. Semaan, E. Mohyeldin, J. Song, C. Bergljung, and S. Jung, "Spectrum for 5g: Global status, challenges, and enabling technologies," *IEEE Communications Magazine*, vol. 56, no. 3, pp. 12–18, 2018.

[2] J. Kurvinen, H. Khknen, A. Lehtovuori, J. Ala-Laurinaho, and V. Viikari, "Co-designed mm-wave and lte handset antennas," *IEEE Transactions on Antennas and Propagation*, vol. 67, no. 3, pp. 1545–1553, March 2019.

[3] R. Rodriguez-Cano, S. Zhang, K. Zhao, and G. F. Pedersen, "Reduction of main beam-blockage in an integrated 5g array with a metal-frame antenna," *IEEE Transactions on Antennas and Propagation*, vol. 67, no. 5, pp. 3161–3170, May 2019.

[4] M. M. Samadi Taheri, A. Abdipour, S. Zhang, and G. F. Pedersen, "Integrated millimeter-wave wideband end-fire 5g beam steerable array and low-frequency 4g lte antenna in mobile terminals," *IEEE Transactions on Vehicular Technology*, vol. 68, no. 4, pp. 4042–4046, April 2019.

[5] M. S. Sharawi, M. Ikram, and A. Shamim, "A two concentric slot loop based connected array mimo antenna system for 4g/5g terminals," *IEEE Transactions on Antennas and Propagation*, vol. 65, no. 12, pp. 6679–6686, Dec 2017.

[6] R. Rodriguez-Cano, S. Zhang, K. Zhao, and G. F. Pedersen, "Mm-wave beam-steerable endfire array embedded in slotted metal-frame lte antenna," *IEEE Transactions on Antennas and Propagation*, 2020.

[7] J. Park, S. Y. Lee, J. Kim, D. Park, W. Choi, and W. Hong, "An optically invisible antenna-on-display concept for millimeter-wave 5g cellular devices," *IEEE Transactions on Antennas and Propagation*, vol. 67, no. 5, pp. 2942–2952, May 2019.

[8] W. Hong, S. Ko, Y. G. Kim, and S. Lim, "Invisible antennas using mesoscale conductive polymer wires embedded within oled displays," in *2017 11th European Conference on Antennas and Propagation (EUCAP)*, March 2017, pp. 2809–2811.

[9] W. Hong, S. Lim, S. Ko, and Y. G. Kim, "Optically invisible antenna integrated within an oled touch display panel for iot applications," *IEEE Transactions on Antennas and Propagation*, vol. 65, no. 7, pp. 3750–3755, July 2017.

[10] J. Park, S. Y. Lee, Y. Kim, J. Lee, and W. Hong, "Hybrid antenna module concept for 28 ghz 5g beamsteering cellular devices," in *2018 IEEE MTT-S International Microwave Workshop Series on 5G Hardware and System Technologies (IMWS-5G)*, Aug 2018, pp. 1–3.

[11] G. John, R. Chatterjee, and S. Chatterjee, "Effects of environment on the surface wave characteristics of a dielectric-coated conductor-part iv," *Journal of the Indian Institute of Science*, vol. 59, no. 1, p. 51, 2013.

[12] S. Y. Lee, D. Choi, Y. Youn, and W. Hong, "Electrical characterization of highly efficient, optically transparent nanometers-thick unit cells for antenna-on-display applications," in *2018 IEEE/MTT-S International Microwave Symposium - IMS*, June 2018, pp. 1043–1045.